Effect of NanoTiO$_2$ Addition on Poly(methyl methacrylate): An Exciting Nanocomposite

Amit Chatterjee[1,2]

[1]*Naval Material Research Laboratory, DRDO, Ambernath, India*
[2]*Center for Composite Material, University of Delaware, Newark, Delaware*

Received 20 August 2009; accepted 25 November 2009
DOI 10.1002/app.31883
Published online 22 February 2010 in Wiley InterScience (www.interscience.wiley.com).

ABSTRACT: A systematic research has been conducted to investigate the matrix properties by introducing nanosize TiO_2 (5 nm, 2.0–30% by weight) filler into a poly (methyl methacrylate) (PMMA) resin. A twin screw extraction process was developed to disperse the particles into the PMMA. The thermal, mechanical, and viscoelastic properties of the virgin PMMA and nanoTiO_2-PMMA composite were measured. The nanofiller infusion improves the thermal, mechanical and viscoelastic properties of the PMMA. Nanocomposite shows increase in storage modulus (~ 60%), rubbery modulus (~ 210%), glass transition temperature (~ 27%), crosslink density (~ 213%), initial decomposition temperature (~ 83% at 1% wt. loss), and activation energy (~ 141%). Mechanical performance and thermal stability of the nanoTiO_2-PMMA composites are depending on the dispersion state of the TiO_2 in the PMMA matrix. Scanning electron microscopic study shows that the particles are well dispersed in the PMMA matrix. They are correlated with loading. Kinetics for thermal degradation analysis was studies. The integral procedural decomposition temperature (IPDT) is enhanced (~ 117%). The nanocomposites of high activation energy possess high thermal stability. Interrelation of T_g, crosslink density, IPDT, storage modulus, activation energy, and TiO_2 weight percent are established. Various reasons for these effects in terms of reinforcing mechanisms have been discussed. © 2010 Wiley Periodicals, Inc. J Appl Polym Sci 116: 3396–3407, 2010

Key words: PMMA; TiO_2; nanocomposite; DMA; TGA; kinetics

INTRODUCTION

Incorporation of inorganic nanoparticles into a polymer matrix can significantly affect the properties of the matrix.[1–3] The obtained composites might exhibit improved thermal, mechanical or optical properties. These hybrid materials couple the structural flexibility and the convenient processing of the polymers with the high carrier mobility, band gap tenability, thermal and mechanical stability of the inorganic component, resulting in synergic effect on their individual properties. Hence, they can allow a versatile design of their physical and chemical properties, to meet the needs of the final end user applications.[4–6] The properties of polymer nanocomposites depend on the type of incorporated nanoparticles, their size and shape, concentration, and interactions with the polymer matrix.[7–9] The main problem in polymer nanocomposite technology is the prevention of particle aggregation.

Various nanoparticles are incorporate into the polymer matrix for nanocomposite applications. TiO_2 is one of them because TiO_2 is an inexpensive, nontoxic, and photostable material, which has good optical and photocatalytic properties for many applications. TiO_2 as photocatalysts have been applied in the purification of water and air, in degradation processes of organic pollutants, medical treatment and microorganism photolysis. TiO_2 has been used as a white pigment for many years. It has a high refractive index and possesses the ability to reflect, refract or scatter light more effectively than any other pigment. At the same time, it can be used in a wide variety of application, where ultraviolet protection is required because of its ability to absorb ultraviolet light. The surface of TiO_2 particle is hydrophilic due to the presence of hydroxyl groups.[10] Among polymers, the PMMA is a very interesting for mechanical and optical applications. It is used as optical fibers, optical disks, and lenses[11] for easy possibility and high transparency in the visible range. It has better thermal and mechanical stability. The incorporation of inorganic TiO_2 particle to PMMA for obtaining a modified polymer with new properties, tunable by varying the composition, size and concentration of the TiO_2 embedded inorganic part, and better thermomechanical stability will be valuable for diverse application. The motivation for the present work is the potential use of polymer/TiO_2 nanocomposites as conductive, strong and yet

Correspondence to: A. Chatterjee (chatterjeamit@yahoo.com).

lightweight materials in the civilian space arena, clear polymer, chemical and biological defense, photocatalytic and photovoltaic application.

Reports are available for the TiO_2-nanocomposite that was prepared by *in situ* emulsion polymerization.[12] The PMMA coated TiO_2 nano particles were prepared for the better dispersion and optically clear composite application.[13] The particles were able to absorb the 95% UV light at 210–400 nm wavelength.[13] The TiO_2-PMMA was also used to prepare PMMA-Silica-TiO_2 nanocomposites for optical applications.[14,15] PMMA-TiO_2 composites were used as additives in water-based lubrication processes.[16] The TiO_2-coated plastic optical fiber was considered as light-transmitting medium and substrate for the potential use in photo catalytic environmental purification system.[16] Organic–inorganic PMMA/SiO_2/TiO_2 composite thin films were used for hydrophobicity application.[17] TiO_2 is used as an antiwear behavior with low friction coefficient and meet the lubricant and protection process. TiO_2-PMMA nanocomposite is used for the ultra fast optical nonlinearity measurements[18,19] with 780 nm, 250-fs laser pulses. It is also use as optical waveguide,[19] magnetic recording medium,[20] and semiconductor nanotube formation by a two-step template process, photovoltaic application for as semiconductor materials.[21] However, all are practically used to enhance the optical and dielectric stability. A few are reported to be the mechanical performance improvements using TiO_2 in PMMA. Those literatures are mainly in-site-to polymerization of PMMA in presence of TiO_2. Even Sol gel method was used for TiO_2 formation in the polymerization process of PMMA. Most of the literatures[13–17] indicate the polymerization of MMA to PMMA in the presence of TiO_2. Existing literatures are based to improve the surface of TiO_2 using various processes. So, the surface modified TiO_2 are mainly used to property improvement of matrix. Information are limited for directly mixing of the unmodified TiO_2 (5 nm) in PMMA matrix and to improve the thermal and mechanical performance of PMMA.

In this research, the PMMA polymer was mixed with TiO_2 in a twin screw extruder machine. The influence of the TiO_2 nanoparticles on the PMMA has been investigated. The viscoelastic and thermal property of the nanocomposite was studied. Improvement in properties is reported.

EXPERIMENTAL

Materials and methods

The nano TiO_2 particles are of 5 nm size supplied by Nanostructured and Amorphous Materials (Los Alamos, NM). The properties of the particles were reported previously.[22] The PMMA was used from a USA based company Scientific Polymer Products (Ontario, NY). The molecular weight is 540,000 confirm by gel permeation chromatography (GPC). The density (g/cc): 1.20 (25°C) refractive index: 1.490; inherent viscosity: 1.25; F_p (°F): 572; T_g (°C): 95 and polydispersity is 2.8.

Preparation of thin film polymer-titanium composites using extrusion processing

Required amount of PMMA and TiO_2 were mixed in a beaker. Measurements were all done by weight. After weighing, the mixture of PMMA and TiO_2 was stirred using a wooden stick and well mixed for about 5–10 min. The DACA extruder (DACA Instruments, Santa Barbara, CA) twin screw extruder for thermoplastic processing was turned on and heated to 190°C, which was 10°C above the melting point of PMMA. The extruder's screws were set to turn at a rate of 100 rpm. The mixture was placed into the extruder injector apparatus, which holds approximately 3–4 mL of sample at a time. The sample was allowed to mix in the machine for about 5–6 min, and then extruded out. Extrusions were cut into small pieces and then re-injected into the machine to mix for another 5–6 min. This was repeated several times to get uniform mixture. Scanning electron microscopy (SEM) picture shows the uniform mixing (Fig. 1). The hot press was heated at the same temperature of 190°C. Two flat aluminum plates were cleaned using acetone and then a generous layer of frekote was applied. When the hot press's desired temperature was reached, the extruded sample was placed between the aluminum plates. The aluminum plates were placed into the hot press for a sandwich formation. Two long aluminum blocks were put beside the aluminum plates onto the hot press so that when the hot press was closed, it was only applying a minimal amount of pressure onto the aluminum plates. This was done to let the aluminum plates heat up and allow the extruded sample to being to melt on the plates. Thirty minutes was allowed for the plates to heat up and melt the TiO_2-PMMA samples. The long metal blocks were then removed; hot press was closed, then applying a pressure of 35 tons. The hot press was kept in the clamping position for 30 min. The heat was turned off. Simultaneously the cooling system turned on while the plates still remained clamped. In early trials, not keeping the plates clamped causes the film to be nonuniform, with bubbles on the surface and existing of lots of voids. Once the temperature of the hot press was reached below 40°C, the plates were removed. Cold water was poured over the plates for further cooling. The film was then removed from the plates. A razor blade was used to cut the film into various sizes for analysis.

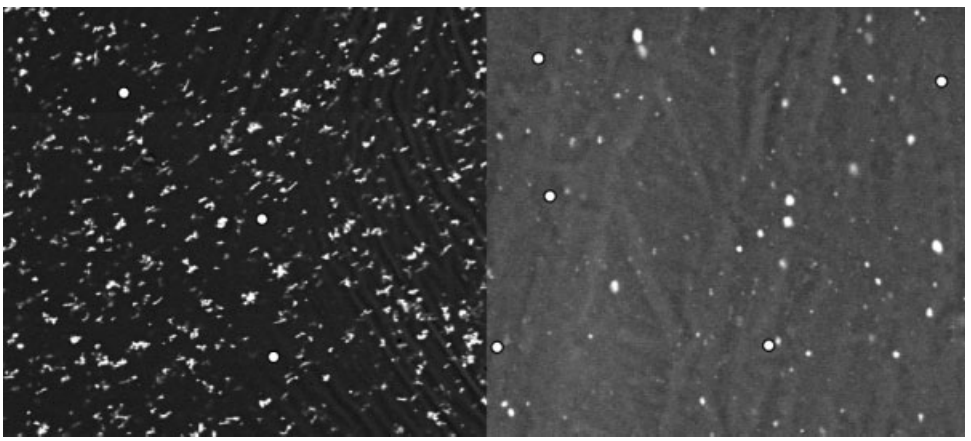

Figure 1 SEM images of TiO_2-PMMA nanocomposites; (a) 10% by wt. of nano TiO_2; (b) 2% by wt. TiO_2.

Characterization techniques

Dynamic mechanical analysis was conducted in a TA (TA Instruments, New Castle, DE) dynamic mechanical analyzer (model DMA 2980) at a frequency of 1 Hz using Film Tension Clamp. The samples were ramped from room temperature (RT) to 250°C using a ramp rate of 2°C/min. The storage modulus and loss modulus were measured. The loss modulus peak is used for measuring the T_g of the resin. The nanocomposite samples were directly cut into rectangular shapes 10.0 × 6.0 × 0.3 mm for DMA analysis.

Thermogravimetric analysis

TGA Q-500 (TA Instruments) was used to measure the degradation properties of the nanocomposites. The experimental parameters used for thermogravimetric analysis (TGA) included a heating rate of 10°C/min, RT to 900°C and a flow rate of helium purging gas is 100 mL/min. The EGA furnace was used for the experiment. The air was also used to oxidative study.

Scanning electron microscopy was conducted in JXA-840 scanning electron microscope. The samples were prepared by gold coating before analysis. The filament voltage was set at 10–30 KV to make an image of the nanostructure.

RESULTS AND DISCUSSION

Morphology

Dispersion of nanoparticles in the PMMA resin is difficult because of the Van Der Waal's force between the nano TiO_2 particles. To optimize the dispersion the time and number of extrusion was varied. The best result was obtained using a total mixing time of 6 min with five times extrusion. SEM analysis was conducted to verify the dispersion quality of the nanocomposite, Figure 1(a,b). We have seen previously that the TiO_2 nanoparticles prior to adding to the PMMA are agglomerated highly.[22] Figure 1(a,b) shows the 10% and 2% TiO2-PMMAnanocomposite images. The particles have been effectively dispersed in the PMMA. Most of the particles are distributed uniformly. However, some residual agglomeration of particles remains, Figure 1. Van Der Waal's force between the particles is the leading reason for weak dispersion of the nano particles in the matrix. The effect of loading on dispersion is also observed. Increasing on loading above 2% creates nonuniformity that clearly observed in the SEM pictures. However, up to 2% loading gives better dispersion with homogeny. Efforts are continuing to focus on improving more homogenous dispersion of the particles in higher concentration.

Performance

Dynamic mechanical thermal properties

Dynamical mechanical tests over a wide range of temperature were performed to see the physical and chemical structural changes of the polymers and the

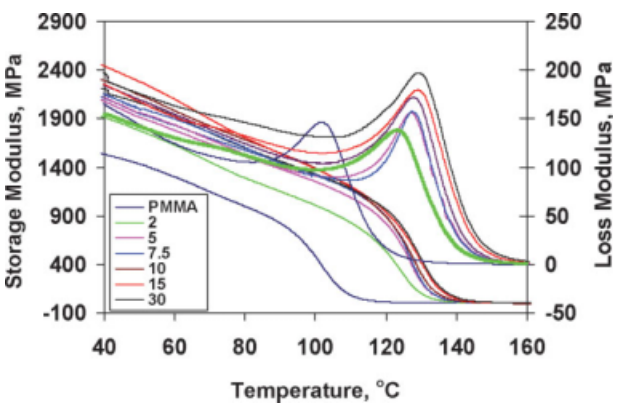

Figure 2 Behavior of storage modulus and loss modulus with temperature for the neat PMMA resin and nanoTiO_2-PMMA composites. [Color figure can be viewed in the online issue, which is available at www.interscience.wiley.com.]

TABLE I
Thermomechanical Properties of PMMA and NanoTiO$_2$-PMMA Composites

Wt % of TiO_2	Loss mod peak, °C	Tan delta, °C	St. mod (MPa) peak, at 40°C	Mod at 115°C (MPa)	Mod at T_g (MPa)	Rub mod (MPa)	Peak area, MPa. min
0	101.5	117	1533	25.6	369	2.67	674
2	123	140	1913	707	382	3.25	710
5	127	140	2078	978	387	4.04	774
7.5	128	142	2110	1055	404	5.00	795
10	128	143	2291	1059	453	5.34	1011
15	129	145	2443	1115	500	7.54	1087
30	128.5	144	2208	1083	515	8.36	1153

nanocomposites. The glass transitions or secondary transitions and yield information about the morphology of polymers were determined. Experimental results of dynamic tests conducted on nanocomposites and neat resin are presented in the Figure 2 from RT to 160°C. In Table I, the storage modulus at different temperatures (40°C, 115°C, at T_g), rubbery modulus, T_g loss modulus peaks and tan delta are noted. Table II represents the percent increased of T_g (loss modulus peak), moduli at 40°C, 115°C and T_g, rubbery modulus, and peak area increased (considering loss modulus peak). The complex moduli for all composites containing fillers are pushed to a higher level relative to the neat resin system. On the other hand the modulus decreases with the temperature rising, but they retain a higher stiffness than the matrix when the temperature exceeds 200°C. The variation of modulus as a function of TiO_2 content is shown in the Figure 2, Table I. The storage modulus of the nanocomposite has been increased with increasing the weight of the TiO_2 content. At 40°C for 15% TiO_2-PMMAnanocomposite, the storage modulus has been increased $\sim$ 60% compared to the virgin PMMA, Table I. The interesting result is shown that the modulus at 115°C has been increased tremendously (2200–4200%) compared to PMMA virgin, Table II. In general, the modulus increased monotonically with the addition of TiO_2 (Fig. 2). However, the rate of increase was greater at lower volume fractions. The trends were similar the absolute values of modulus were higher for nanocomposites fabricated using higher mass. The overall increase in modulus was significant, especially for materials processed at lower concentration. Two percent of the nanocomposite modulus was 35% higher than that for nanocomposites containing 0% TiO_2 by weight (Table I). These improvements in properties are significant considering the increase in weight of the nanocomposites, which is merely 2%. TiO_2 weight fractions >2%, behave like two-phase composites with spheroids having lower aspect ratio. The very nominal increasing rate of modulus improvement (above 10%) may be attributed to the presence of isolated TiO_2 aggregates at higher volume fractions.[22] Because of the high modulus of TiO_2 and the improved interfacial adhesion between nanoparticles and polymer by physiochemical interaction,[20] mechanical load imposed on the nanocomposites transfers through the stronger interfacial surface to the strongest nanoparticles effectively. With increasing the percentage of nanoparticles loading, T_g of the TiO_2-PMMA nanocomposite increases linearly up to 7.5% TiO_2 (3–40%). As the T_g has been increased the modulus peak has been shifted to higher temperature that increased the modulus by 2200-fold (Table I). In most of the cases crosslink density is the key factor of controlling the T_g for normal polymer systems. It increases with enhancement of T_g. So, the

TABLE II
Percent Increased in Thermomechanical Properties of NanoTiO$_2$-PMMA Composites

Wt % of TiO_2	% T_g increased (loss mod peak)	% Modulus (40°C) increased	% Modulus (115°C) increased	% Modulus at T_g increased	% of rubbery modulus increased	% of peak area increased (considering loss mod peak)
0					0	
2	21.2	24.8	2662	3.52	21.6	5.34
5	25.1	35.6	3720	4.88	51.0	14.8
7.5	26.1	37.6	4021	9.49	86.9	17.9
10	26.1	49.4	4037	22.8	99.8	50
15	27.1	59.4	4255	35.5	182	61.3
30	26.6	44.0	4130	39.6	213	71.1

TABLE III
Kinetic Data for NanoTiO_2-PMMA Composites (Activation Energy, IPDT, Crosslink Density, mol. wt. Between Crosslink)

TiO_2 %	Ea; kJ/mol Coats-Redfern	Ea; kJ/mol Horowitz-Metzger	IPDT, °C	Crosslink density, mol/m^3	Mol wt. between crosslink, g/mol
0	64	84	435	393	3054
2	89	108	450	478	2623
5	113	132	519	593	2144
7.5	119	138	548	735	1903
10	154	164	600	785	1865
15	148	165	639	1108	1440
30	146	162	711	1229	1624

crosslink density V_e has been measured. It is obtained using the theory of rubber elasticity from the following equation:[22,23]

$$E' = 3VeRT \quad (1)$$

E' is the storage modulus in the rubbery plateau region, R is the gas constant, and T is the absolute temperature. The values are in Table III. It increases with nano addition. The increased in crosslink density clearly correlated with the incremental in modulus of the nanocomposite due to TiO_2 nano addition. The molecular weight between the crosslink is calculated. The M_C is the average molecular weight per unit volume of the polymer between crosslinks is given by the eq. (2):[22,24]

$$Ve = \rho_p N_A / M_C \quad (2)$$

Where ρ_p is the polymer density, N_A is Avogadro's number and V_e crosslink density in a perfect network. It is observed that the molecular weight between the crosslink decreases with increasing the nano addition (Table III). The modulus at T_g for the nanocomposites has been also increased (Tables II and III) compared to PMMA. The rubbery modulus is increased $\sim$ 212% than the pure PMMA. Amplified in modulus and T_g clearly indicates that the TiO_2 has chemical and physical interaction with the matrix PMMA. The side chain of the methyacralate group has chemical bonding with the TiO_2. The hydrogen bonding with the surface –OH for the TiO_2 with methyacralate will not be ruled out. The TiO_2 can react with –COOR group of PMMA polymer in two different schemes. One scheme is to form H-bond between carbonyl group and surface hydroxyl group of TiO_2. Another scheme is that TiO_2 can be bound with two oxygen atoms of COOR by a bidentate coordination to Ti^{4+} cation. As a result, when TiO_2 come to the surface of the polymer PMMA it will form crosslink structure and bound to the PMMA. This bonding increases with increasing TiO_2 loading as number of particles increases with loading. TiO_2 generally synthesized through Sol-gel method from Ti-compounds. The existence of the surface –OH is most probable and this is confirmed by the FTIR at 3000–3600 cm^{-1}. Many research articles have confirmed the presence of surface hydroxyl group in TiO_2. Therefore, the hydrogen bonding between the –OH group of TiO_2 and the C=O group of methyacralate is taking place. The Ti—O—C bonds through crosslinking between the TiO_2 and PMMA is feasible and has been confirmed by FTIR (Fig. 3). The increased in crosslink density with TiO_2 increment has been further confirm the chemical linkage of TiO_2 and PMMA that increases the modulus value. The TiO_2-PMMA system behaves as a pseudothermoset system. Most likely three dimensionally crosslinked network structure has been formed. So, the mechanical performance of the nanocomposites has been increased. Enhance in T_g may be attributed to a loss in the mobility of chain segments of the PMMA systems resulting from the nanoparticle/matrix interaction.

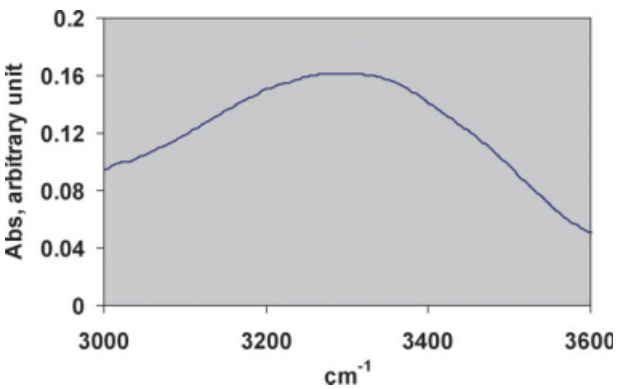

Figure 3 FTIR spectra of pure nano TiO_2; 5 nm, from 3000 to 3600 cm^{-1}. [Color figure can be viewed in the online issue, which is available at www.interscience.wiley.com.]

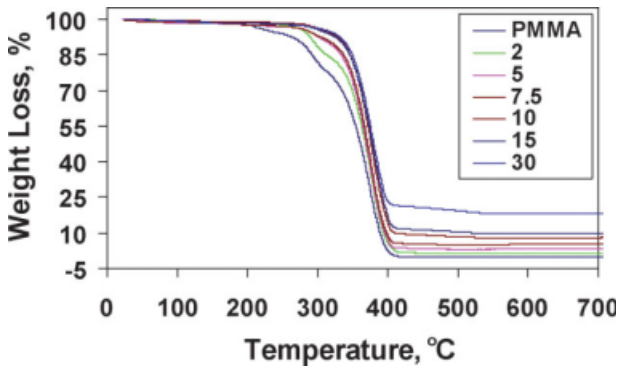

Figure 4 TGA thermograms for the virgin PMMA and nanoTiO$_2$-PMMA composites (2–30%) with temperature. [Color figure can be viewed in the online issue, which is available at www.interscience.wiley.com.]

Impeded chain mobility is possible if the nanoparticles are well dispersed in the matrix. The particle surface-to-surface distance should then be relatively small and chain segment movement may be restricted. Good adhesion of nanoparticles with the surrounding polymer matrix would additional benefit the dynamic modulus by hindering molecular motion to some extend. The hard particles incorporated into the polymer would act as additional virtual network nodes. Hence, the enhancement of this T_g is due to the incorporation of nanoparticles. The enhanced glass transition temperature is related to the restriction effect of the TiO_2 on segmental motion. The TiO_2 chemically reacts with the PMMA. Interfacial layers formed during interaction process will exhibit a significantly different segmental dynamics from the bulk resin. Therefore, TiO_2-PMMA-nanocomposite has exhibited a higher T_g than the corresponding neat resin system. The peak temperature in the loss modulus tends to shift to higher temperatures with increasing loading. On the other hand, the restriction effect of segmental motion is also manifest by the change in peak width of the loss modulus. According to the coupling model theory suggested by Roland and Ngai,[22] the segmental motion of polymers below T_g is a cooperative process and has to overcome the resistance from the surrounding segments to accomplish the transformation between configurations. As more segments are restricted by the presence of TiO_2, the activation threshold for the motion of some segments becomes higher. As a consequence, the loss modulus peak during the glass transition trends to become wider with increasing restriction effect. The restricted segmental motion observed herein not only causes an increase in the T_g and modulus but also improves the dimensional stability of the polymeric materials. For the polymeric materials, dimensional stability is closely related to the chemical structure of the molecular chains and the topological structure formed. To change in the stiffness of primary chains, one can adjust the response of segment motions to the change in surroundings temperature.

Thermal stability of nanoTiO$_2$-PMMA composite

The TGA was done by nonisothermal process. It is done to understand the thermal stability, measured in terms of the onset temperature of degradation, of the nanophase composite system. The real-time characteristic curves were generated using the Universal Analysis Data Acquisitation System (TA Instruments, New Castle, DE). It is given by initial decomposition temperature, temperature of maximum rate of weight loss (T_{max}), integral procedural decomposition temperature (IPDT), and activation energy for decomposition. The TGA and DTG curves obtained for the pure PMMA and PMMA-TiO_2 composite samples are shown in Figures 4 and 5. Table IV represents the data for 1%, 5%, 50%, and 95% weight loss, char content, and peak decomposition temperatures for the neat PMMA and nanoTiO$_2$-PMMA composite. The thermal stability of the nanocomposite increases with nano TiO_2 loading. The 5% weight loss for the neat PMMA, 2%, 5%, 7.5%, 10%, 15%, and 30% TiO_2-PMMA-nanocomposite are occurred at 235°C, 281°C, 288°C, 289°C, 314°C, 307°C, and 317°C, respectively, Figures 4 and 5, Table IV. Researchers are commonly considered 50% weight loss as an indicator for structural destabilization.[25] So, in the present study 50% of the total weight loss is considered as the structural destabilization point of the system. It is clearly observed that the neat resin sample without TiO_2 nanoparticles is stable up to 134°C (1% weight loss Table IV), where as with 2% TiO_2 loading the composite is stable up to 154°C, Table IV. The thermal stability drop down to 235°C (5% weight loss). Figure 6 shows the increased in thermal stability (1%, 5%, 50%, and 95% weight loss) with % TiO_2 loading for nanoTiO$_2$-

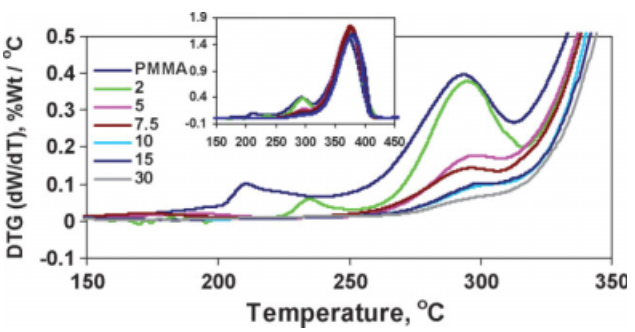

Figure 5 DTG curves of pure PMMA and nano TiO_2-PMMA composites with varying percent of TiO_2 contents. Insert: full scale graph. [Color figure can be viewed in the online issue, which is available at www.interscience.wiley.com.]

TABLE IV
TGA Analysis (Decomposition Temperatures, Temperature of Maximum Rate of Weight Loss, Char Content) for PMMA and NanoTiO$_2$-PMMA Composites

Wt % of TiO_2	Temperature, °C at % weight loss started				Residue, %	Maximum decomposition temperature, °C (area, % min/°C)	Second decomposition, °C (area, % min/°C)	Third decomposition temperature, °C (area, % min/°C)
	1%	5%	50%	95%				
0	134	235	359	395	0	374 (6.24)	292 (0.578)	210 (0.103)
2	154	281	366	402	1.75	375 (7.105)	294 (0.661)	235 (0.05)
5	180	288	368	404	3.42	375 (7.623)	296 (0.071)	
7.5	181	288	370	488	5.5	375 (7.716)	292 (0.047)	
10	201	314	375		8.22	378 (7.804)	302 (0.004)	
15	258	307	377		11.8	379 (7.50)	302 (0.001)	
30	246	317	379		18.2	378 (7.31)	302 (0.001)	

PMMA composite. Nanoparticle loading (2–15%) increases the thermal stability of the PMMA. Further increment in particle loading decreases the thermal stability, 30% (Table IV, Figure 4). The TGA measurement shows at 395°C the neat resin has 5% char content. However, for 5% TiO_2-PMMA-nanocomposite system about 10% char weight is present at 395°C (Figure 4). Generally, polymer having higher crosslink density shows higher maximum decomposition temperature.[26] The crosslink density is increased with loading (Table III). It may be one of the causes to increase the decomposition temperature of the nanocomposite. The crosslink density is maximized when the complete stoichiometry of the PMMA is maintained. The decomposition temperatures are increased with increase in %TiO_2 loading (Figures 4 and 5). Increment in decomposition temperature with TiO_2 loading is due to the barrier formation of heat and oxygen in the PMMA matrix by ceramic nature of the particles. The retardant effects of the composite to heat and oxygen in the PMMA matrix are strengthened when the TiO_2 loading increases. As the number of the particles is increased with loading, further enhancement of loading (>10%) causes particle-to-particle interaction domination than the particle-to-matrix interaction. The defect due to agglomeration increases with loading and shows the less retardant effects to heat and oxygen, but till higher and increases with TiO_2 loading. The reason for not changing of the temperature significantly above 10% by weight of TiO_2-PMMA systems is due to (macroscopically) simple colligative thermodynamics effect of an impurity on a bulk solution. Microscopically, it may be seen as the result of the perturbation that the TiO_2 introduces to the three-dimensional structure of the polymer. This perturbation weakens the Van Der Waal's interaction between the polymer chains. This affects the stability for the polymer, and reflected in the thermal stability. This perturbation begins at a point when the number of particle reaches a certain level and particle-to-particle interaction initiates leading to agglomeration of particles into lumps, which acts as an impurity in the system.[22]

It is well known that PMMA thermally decomposes by depolymerization.[27] The thermal stabilization of free radically polymerized PMMA is significantly affected by the presence of unsaturated end groups and head-to-head bonds obtained during termination by disproportionation and combination respectively. The thermal degradation of free radically polymerized PMMA occurs in three stages, characterized by three maxima in the differential thermal analysis (DTA) curve at about 180°C, 300°C, and 380°C at a heating rate of 10°C/min.[28–30] However, we obtained 210°C, 294°C, and 374°C (Table IV). These stages have been attributed to different modes of initiation of depolymerization. The first peak corresponds to depolymerization initiated by the scission of the weak head-to-head bonds and the

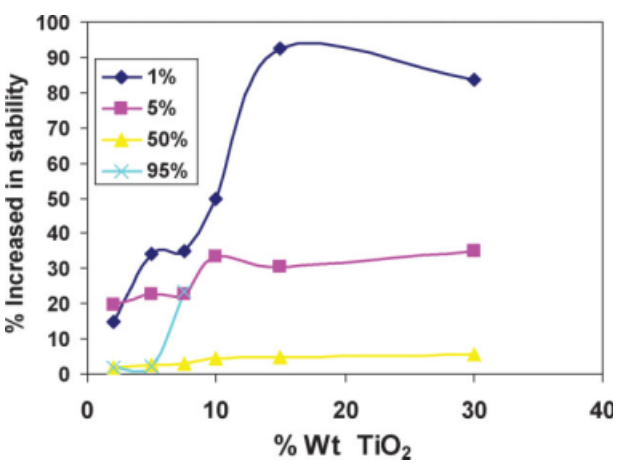

Figure 6 Increased in thermal stability of the nanoTiO$_2$-PMMA composites with percent of NanoTiO$_2$ loading. [Color figure can be viewed in the online issue, which is available at www.interscience.wiley.com.]

second one corresponds to depolymerization initiated by the unsaturated vinyl chain ends. The third peak corresponds to depolymerization initiated by random main chain scission. This DTG peaks is typical for anionically polymerized PMMA, which does not contain head-head bonds or unsaturated chain end groups. DTA curve of pure PMMA sample exhibits three peaks at 210°C, 294°C, and 374°C correspond to three different modes of initiation of depolymerization of free radically polymerized PMMA (Figure 5). The thermal degradation of PMMA-TiO_2 samples occurs in two stages, and their DTA curves show two peaks (Figure 5). The most intense DTA peak for all investigation samples is approximately at 380°C, which corresponds to depolymerization initiated by random chain scission. The first peak near 180°C is obtained for the pure PMMA and the 2% composite samples. However, rest of the samples did not show the first decomposition peak. That indicates the increment in stability of PMMA with addition of TiO_2. Even in 2% TiO_2 the peak area and height are much lower than the pure PMMA sample (Table IV). DTA curves of the TiO_2-nanocomposite samples do not contain peak at 180°C indicating the lack of head-to-head bonds in PMMA chains. The DTA peak originating from depolymerization initiated by unsaturated vinyl end is much less pronounced and shifted to higher temperature for the nanocomposite samples compared to PMMA. In this stage of thermal degradation, mass loss of PMMA/TiO_2 samples decreases with increasing content of the TiO_2 particles. This indicates the number of polymer chains with double bond at the end decreases with increasing content of these particles. The results can be explained by the assumption that TiO_2-particles react as radical scavengers and/or chain-transfer agents during the polymerization. This is in agreement with the work of Kashiwagi et al.[28] who showed that the first two DTA maxima could be decreased or completely suppressed when PMMA was synthesized in the presence of the chain-transfer agent tetra-butyl mercaptan. The result with TiO_2-PMMAnanocomposite shows the same trend. The first two peaks disappeared for the 10 and above weight percent of the TiO_2. The peak area decreased with increased TiO_2 content and the final decomposition peak area has been increased with increased of TiO_2 and up to 10% is maximum than it has been decreased with further increment of TiO_2. So, the TiO_2 act as a chain transfer agent and that increases the thermal stability of the nanoTiO$_2$-PMMA composite.

Kinetics for thermal degradation

To evaluate the thermal stability more detailed, nonisothermal thermal degradation kinetics were calculated. The apparent conversion, α, is defined as the ratio of the actual weight loss to the total weight loss,

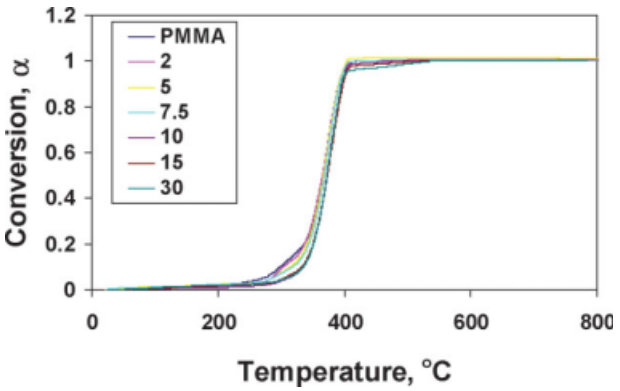

Figure 7 Conversion curves for nanoTiO$_2$-PMMA composites. [Color figure can be viewed in the online issue, which is available at www.interscience.wiley.com.]

$$\alpha = (m_0 - m)/(m_0 - m_\infty)$$

m is the actual weight at time t (or at temperature T); m_0 the initial weight, and m_∞ is the weight at the end of nonisothermal experiments. Figure 7 shows the conversion plot. Consequently, the rate of degradation $d\alpha/dt$ for an n-order reaction, depends on the temperature and the weight of sample, as given by eq. (3)

$$\frac{d\alpha}{dt} = k(1-\alpha)^n \tag{3}$$

where α is the apparent conversion, k is the rate constant given by the expression:

$$k = A\mathrm{e}^{-\frac{E}{RT}} \tag{4}$$

where A is the Arrhenius frequency factor and E is the apparent activation energy. For a linear heating rate say ϕ degree/min:

$$\phi = dT/dt \tag{5}$$

So in dynamic mode, the rate expression can be written as:

$$\frac{d\alpha}{(1-\alpha)^n} = \frac{A}{\phi}\mathrm{e}^{-\frac{E}{RT}}dT \tag{6}$$

where α at temperature T depends on the heating rate ϕ. It was assumed that the temperature of maximum deflection in differential thermal analysis is also the temperature at which the reaction rate is a maximum. The maximum rate occurs when the derivative is zero. Different kinetics expressions could be obtained by integrating the above equation with different

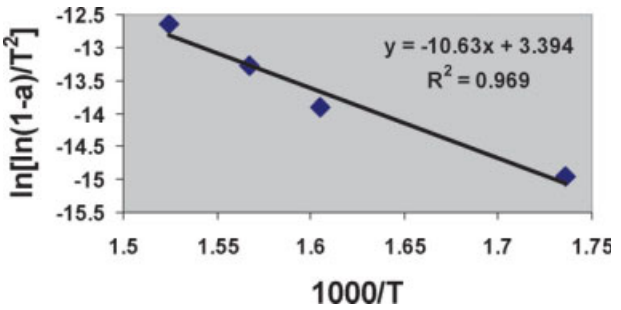

Figure 8 Kinetics of thermal decomposition of PMMA nanocomposites (2.0% TiO_2 by wt) by using Coats-Redfern Equation. [Color figure can be viewed in the online issue, which is available at www.interscience.wiley.com.]

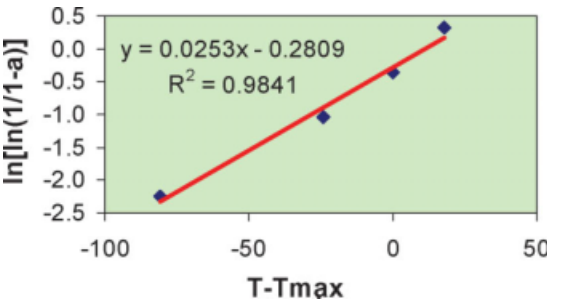

Figure 9 Kinetics of thermal decomposition of PMMA by using Horowitz–Metzger Method. [Color figure can be viewed in the online issue, which is available at www.interscience.wiley.com.]

approximation treatments. Among those kinetics equations, the Coats-Redfern equation[22,31] is one of the well-known models, commonly used and are as follows:

$$\ln\left[\frac{1-(1-\alpha)^{1-n}}{(1-n)T^2}\right] = \ln\left[\frac{AR}{\phi E}\left(1-\frac{2RT}{E}\right)\right] - \frac{E}{RT} \quad (7)$$

where $n \neq 1$.

If the order of reaction, n is equal to one ($n = 1$), in which case the solution of eq. (6) after taking the log become:[31]

$$\ln\left[\frac{\ln(1-\alpha)}{T^2}\right] = \ln\left[\frac{AR}{\phi E}\left(1-\frac{2RT}{E}\right)\right] - \frac{E}{RT} \quad (8)$$

For the decomposition of PMMA, the mechanism of random scission of molecules dominates. Therefore, the decomposition could be treated as one order reaction. The curves of $\ln(1-\alpha)$ versus $1000/T$ were computed with conversion. The activation energy was calculated from the slope of the line. Figure 8 shows the Coats-Redfern curve treated with one order reaction. The apparent activation energies are tabulated in Table III.

Energy of activation for decomposition of PMMA-nanocomposite is also calculated from TGA curves by the integral method of Horowitz and Metzger[22] according to the following equation:

$$\ln\left[\ln\left(\frac{1}{1-\alpha}\right)\right] = \left[\frac{E_a\phi}{RT^2{}_{\max}}\right] \quad (9)$$

where α is the decomposed fraction, E_a the activation energy for decomposition, T_{max} the temperature at maximum rate of weight loss, $\theta = T - T_{max}$ and R the universal gas constant. From the plot of $\ln\left[\ln\left(\frac{1}{1-\alpha}\right)\right]$ versus θ, Figure 9, the activation energy for decomposition was calculated from the slope of the straight line in eq. (9). The calculated activation energy as a function of TiO_2 loading is tabulated in Table III. Incorporation of TiO_2 into PMMA would promote the thermal stability of PMMA resin (Table III). The E_a has increased tremendously (140%) from the neat polymer (Table III). It reached a highest at 10% TiO_2 loading and decreased with addition of TiO_2. The cause of increased and decrease of E_a is the perturbation, particle agglomeration and particle–matrix interaction theories as decreased previously. In addition, thermal stability has also been characterized by given IPDT. IPDT has been correlated the volatile parts of polymeric materials and used for estimating the inherent thermal stability of polymeric materials. Figure 10 shows the schematic diagram of Doyle's proposition for determining the IPDT of a major factor on thermal stabilities of the samples. The IPDT is calculated as follows:

$$\text{IPDT}(^\circ\text{C}) = A^*K^*(T_f - T_i) + T_i \quad (10)$$

$$A^* = (A_1 + A_2)/(A_1 + A_2 + A_3) \quad (11)$$

$$K^* = (A_1 + A_2)/A_1 \quad (12)$$

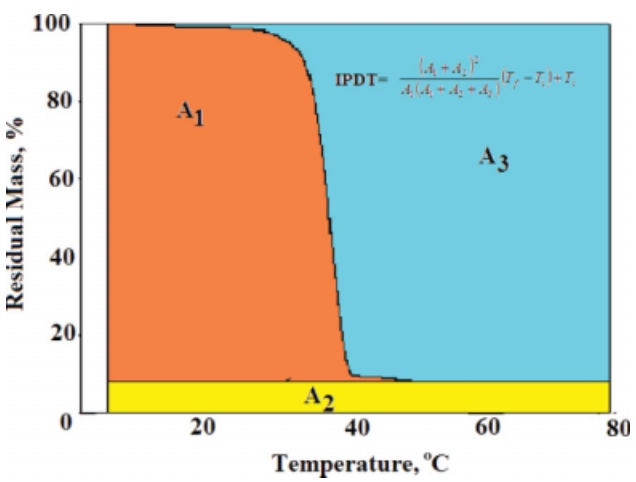

Figure 10 Schematic representation of A_1, A_2, A_3, A*, and K* for Doyle's Diagram. [Color figure can be viewed in the online issue, which is available at www.interscience.wiley.com.]

TABLE V
Correlation Potential of Crosslink Density, % TiO_2, Storage Modulus, Glass Transition Temperature, Ea, IPDT and Mol. Wt. Between the Crosslink for NanoTiO_2-PMMA Composites

Correlation parameters	Equation	Correlation coefficient, R^2
Crosslink density, mol/m^3 versus % TiO_2	$Y = -0.99X^2 + 59.1X + 358$	0.975
Ea kJ/mol, versus mol. wt. between the crosslink, g/mol	$Y = -0.04X + 209$	0.930
Ea kJ/mol, versus crosslink, density, mol/m^3	$Y = -0.0002X^2 + 0.41X - 44.8$	0.957
Ea kJ/mol, versus % TiO_2	$Y = -0.2282X^2 + 9.40X + 68.5$	0.941
Storage modulus, MPa, versus crosslink density, mol/m^3	$Y = -0.0027X^2 + 5.11X + 97.2$	0.902
T_g, °C, versus Ea, kJ/mol	$Y = -0.0068X^2 + 2.01X - 17.9$	0.968
IPDT, °C, versus crosslink density, mol/m^3	$Y = 0.3132X + 319$	0.957
IPDT, °C, versus mol. wt. between the crosslink, g/mol	$Y = -0.1592X + 890$	0.821
IPDT, °C, versus Ea, kJ/mol	$Y = 2.907X + 161$	0.828
IPDT, °C, versus % TiO_2	$Y = -0.3336X^2 + 19.5X + 426$	0.992
IPDT, °C, versus storage modulus, MPa	$Y = -0.0223X^2 + 27.5X - 5993$	0.868
T_g, °C, versus storage modulus, MPa	$Y = -4E\text{-}05X^2 + 0.212X - 129$	0.988
Mol. wt. between the crosslink, g/mol versus % TiO_2	$Y = 3.8877X^2 - 161X + 2964$	0.978
T_g, °C, versus % TiO_2	$Y = -0.0657X^2 + 2.53X + 111$	0.663
T_g, °C, versus crosslink density, mol/m^3	$Y = -8E\text{-}05X^2 + 0.154X + 60.4$	0.764
T_g, °C versus IPDT, °C	$Y = -0.0006X^2 + 0.717X - 92.6$	0.667

where, A^* is the area ratio of total experimental curve defined by the total TGA thermogram, T_i and T_f are the initial and final experimental temperatures, respectively. The A_1, A_2, and A_3 are the areas under the TGA curve and are shown in Figure 10. These areas are used for calculating A^* and K^*. So, the

$$\text{IPDT} = \frac{(A_1 + A_2)^2}{A_1(A_1 + A_2 + A_3)}(T_f - T_i) + T_i \qquad (13)$$

The relationship between IPDT and the TiO_2 loading is shown in Tables III and V. The changes in activation energy of the nanocomposites may be the structural evolution. In minimum loading, the particle–matrix distribution is homogeneous in nature. The ceramic particles block the heat as it is insulator as described previously. Heat and oxygen movement paths are lingering due to the presence of the ceramic particles. So, the retardant effects to heat and oxygen are observed and that enlarged further with loading, since the number of nano particles increases (up to 10%). Additional increment of loading causes detrimental effect due to the agglomeration of particles. Agglomerated particles are nonuniformly distributed in the matrix and are less effective to blocking the heat and oxygen.

The IPDT trend is same as for the evolution of the activation energy. It increases monotonically with nano loading. This may be the same physic natures of activation energy and IPDT. The activation energy describes the fast decomposition process of the resin network, ignoring the initial decomposition and char yield formation (Table III). IPDT, however, reflects the whole stability of the sample, including the initial, fast decomposition and final (char forming) steps. As the TiO_2 in the PMMA matrix mainly contributes the retardant effects to heat and oxygen and char formation, the IPDT increases with TiO_2 loading. However, the activation energy reaches a maximum at 10% loading because the dispersion state of the TiO_2 is the main concern in determining the fast decomposition process of the PMMA resin. It is found that the TiO_2 lead to a lower degradation of the crosslink composites at higher temperature than pure PMMA ones. The composites with TiO_2 have significantly increased E_a. TiO_2 is reacting with PMMA leading to an increase of crosslink density of the composites, resulting in increased the E_a, thermal stability, as seen in Table III. The result is mainly due to the formation of a compacted crosslink structure of the composites.[32]

Table V shows the dependences of the storage modulus and the activation energy for decomposition (E_a) of the composites on the crosslink density (V_e). As a result, it is found that the crosslink density of the composites is largely correlated with the modulus (regression coefficient, $R = 0.90$) and the E_a (regression coefficient, $R = 0.96$) of the TiO_2 composites. It is recognized that increasing V_e plays a major role in improving the mechanical interfacial properties and thermal stabilities of the TiO_2-PMMA composites. The activation energy of thermal degradation generally increases with the extent conversion for different contents of TiO_2. Increasing dependencies of the activation energy on conversion are quite typical for degradation of polymers, including PMMA materials. The thermal stability of nanocomposite increases with the degree of conversion. The formed char protects the polymer from further degradation. Owing to the low surface energy of TiO_2, it

would result in migration to the surface of resins to form a heat-resistant layer discussed previously.

The correlation between the crosslink density, T_g, %TiO_2 and storage modulus are composed (Table V). Correlation, correlation coefficient and equations for T_g, E_a, storage modulus, IPDT, crosslink density, molecular weight between crosslink and %TiO_2 for TiO_2 and nanoTiO_2-PMMA composite are tabulated in Table V. The T_g of the nanocomposite amplified up to 7.5% TiO_2 addition and stays unaffected after further increment. However, the crosslink density increases with %TiO_2 (30%). A second order polynomial correlation between the crosslink density and %TiO_2; $y = -0.9901 \times 2 + 59.137x + 358.22$; $R^2 = 0.9753$; is found. T_g and crosslink density have no such correlation. Initially the crosslink density increases as T_g increases with nano addition (7.5%) and after it is increased but T_g remained unchanged (within experimental error). IPDT has been correlated with crosslink density (Fig. 11). The correlation equation is $Y = 0.3132X + 319$, correlation coefficient $R^2 = 0.9567$. E_a and IPDT increases with nano addition (Tables III and V). Percent increased of E_a and IPDT with nano addition is presented in Figure 12. E_a and IPDT increase $\sim$ 120%. A second order polynomial correlation is found (Table V) between the E_a and %TiO_2. Second order polynomial correlations are also found for molecular weight between the crosslink and %TiO_2; storage modulus and crosslink density; T_g and storage modulus; IPDT and storage modulus; IPDT and %TiO_2, T_g and E_a; E_a and crosslink density and E_a versus %TiO_2, Table V. The correlation factor is in between 0.99 and 0.87. The linear relationship is observed for the E_a and molecular weight between the crosslink (Table V); IPDT and crosslink density (Fig. 11); IPDT and molecular weight between the crosslink; IPDT and E_a as well (Table V). The correlation factor (R^2) is in the range

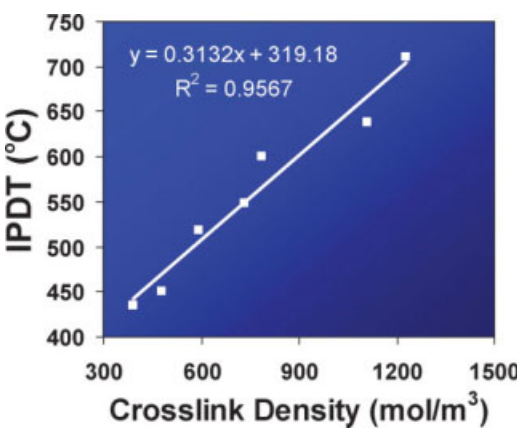

Figure 11 Correlation between IPDT with crosslink density of the nanoTiO_2-PMMA Composites. [Color figure can be viewed in the online issue, which is available at www.interscience.wiley.com.]

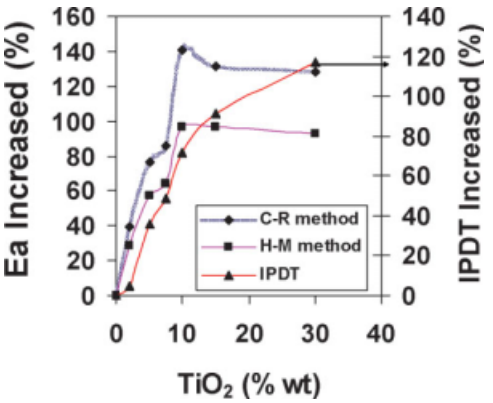

Figure 12 Effect of TiO_2 loading on % increased in activation energy (calculated by using Horowitz–Metzger method, Coats-Redfern method) and % increased in integral procedural decomposition temperature (IPDT). [Color figure can be viewed in the online issue, which is available at www.interscience.wiley.com.]

of 0.96–0.82 for the systems. The correlation between measured parameters for the nanocomosites can be used to predict each other if one of them is known. Therefore, the generated equations can be used to predict the viscoelastic properties of the nanoTiO_2-PMMA composite.

CONCLUSIONS

The nanoTiO_2-PMMA composite was prepared by mixing various weight percent of the TiO_2. Incorporation of TiO_2 improves the thermal, mechanical and viscoelastic properties of the PMMA. The glass transition temperature was improved by 30% with addition of 5% TiO_2. Presence of TiO_2 leads the T_g improvement due to chemical and mechanical interlocking of the materials. The thermal stability was improved. Superior in thermal stability is due to inhibiting effects of the TiO_2 particles on degradation stages for the thermo-oxidative degradation of PMMA. FTIR characterization shows the chemical interaction of the TiO_2 with PMMA and that improves the performance.[33] The developed TiO_2-PMMA nanocomposite has vast application and can be used for property improvement of PMMA using very low amount of TiO_2 (2%).

References

1. Dzunuzovic, E.; Jeremic, K.; Nedeljkovic, J. M. Eur Polymer J 2007, 43, 3719.
2. Beecroft, L. L.; Ober, C. K. Chem Mater 1997, 9, 1302.
3. Gangopadhyay, R.; De, A. Chem Mater 2000, 12, 608.
4. Convertino, A.; Leo, G.; Tamborra, M.; Sciancalepore, C.; Striccoli, M.; Curri, M. L.; Agostiano, A. Sens Actuators B Chem 2007, 126, 138.
5. Judeinstein, P.; Sanchez, C. J. Mater Chem 1996, 6, 511.
6. Caseri, W. Macromol Rapid Commun 2000, 21, 705.

7. Yuwono, A. H.; Liu, B.; Xue, J.; Wang, J.; Elim, H. I.; Ji, W. J Mater Chem 2004, 14, 2978.
8. Lu, S. R.; Zhang, H. L.; Zhao, C. X.; Wang, X. Y. Polymer 2005, 46, 10484.
9. Pandey, J. K.; Reddy, K. R.; Kumar, A. P.; Singh, A. P. Polym Degrad Stab 2005, 88 234.
10. Erdem, B.; Hunisicker, R. A.; Simmons, G. W.; Sudol, E. D.; Dimonie, V. L.; El-Aasser, M. S. Langmuir 2001, 17, 2664.
11. Hornak, H. A. In Polymers for Lightwave and Integrated Optics; Marcel Dekker: New York, 1992, 45 p.
12. Wang, I.; Xu, R.-F.; Ding, X.-J. Ziran Kexueban 2006, 33, 72.
13. Mingjiao, Y.; Dan, Y. Colloid Polym Sci 2005, 284, 243.
14. Wenbin, H.; Marco, B.; Galen, S. In Transparent PMMA-Silica-TiO$_2$ Nanocomposites for Optical Applications; American Chemical Society: Washington, DC, CODEN 69FGKM, AN 2004, 225726.
15. Wencao, G.; Feng, W.; Zhanjun, G. Ziran Kexueban 2003, 31, 108.
16. Hongdae, S.; Hyunku, J. Mater Sci Forum 2003, 439, 34.
17. Guotuan, G.; Zhijun, Z.; Hongxin, D. Appl Surf Sci 2004, 221, 129.
18. Elim, H. I.; Yuwono, A. H.; Xue, J. M.; Wang, J.; Ji, W. Condens Matter 2003, 1, 12.
19. Wei, M.-H.; Chen, W.-C. Polymer Prepr 2002, 43, 95.
20. Handa, M.; Tojo, M.; Osawa, T. Eur Pat Appl EP0879695, (1998).
21. Heishoku, A.; Yutaka, H.; Ryutoku, Y. Zairyo 1993, 42, 1345.
22. Chatterjee, A.; Islam, M. S. Mats Sci Eng A 2008, 487, 574; and references cited therein.
23. Nielson, L. E.; Landel, R. F. Mechanical Properties of Polymers and Composites, 2nd ed.; Marcel Dekker: New York, 1994.
24. Flory, P. J. J. Chem. Phys 1950, 18, 108.
25. Mathew, A. P.; Packirisamy, S.; Thoms, S. Polym Degrad Stab 2001, 72, 423.
26. Horowitz, H. H.; Metzger, G. Anal Chem 1963, 35, 1464.
27. McNeill, I. C. Eur Polym J 1968, 4, 21.
28. Kashiwagi, T.; Inaba, A.; Brown, J. E.; Hatada, K.; Kitayama, T.; Masuda, E. Macromolecules 1986, 19, 2160.
29. Popovic, I. G.; Katsikas, L.; Weller, H. Polym Bull 1994, 32, 597.
30. Popovic, I. G.; Katsikas, L.; Muller, U.; Velickovic, J. S.; Weller, H. Macromol Chem Phys 1994, 195, 889.
31. Coats, A. W.; Redfern, J. P. Nature 1964, 201, 68.
32. Kwak, G. H.; Park, S. J.; Lee, J. R. J Appl Polym Sci 2000, 78, 290.
33. Chatterjee, A. unpublished results, 2009.